

of the Fermi level. We write

$$\epsilon_1 = \left(\frac{\hbar^2}{2m} \right) (k_n^2 + k_b^2 + k_c^2), \quad (77)$$

$$Y \sim \int dk_b dk_c \rho(\epsilon_2) d\epsilon_2 \sim (E - E_F)^2. \quad (78)$$

6. Discrete Imperfection States

If the imperfection states are localized in energy at the value $-E_L$ below the Fermi level, the yield will be

$$\eta \sim (E - E_L).$$

ACKNOWLEDGMENTS

The author would like to acknowledge a great deal of stimulating discussion with G. W. Gobeli and F. G. Allen.

Direct and Indirect Excitation Processes in Photoelectric Emission from Silicon

G. W. GOBELI AND F. G. ALLEN
Bell Telephone Laboratories, Murray Hill, New Jersey
(Received February 23, 1962)

The spectral dependence of saturation photoelectric emission has been studied for atomically-clean (111) silicon surfaces which were prepared by cleavage in high vacuum. The observed spectra, and their dependence on sample doping, are interpreted as being due to a volume excitation process which is modified by space charge band bending effects. Both direct and indirect optical excitation thresholds are observed, at 5.45 eV and 5.15 eV, respectively, with the latter being equal to the electron affinity, χ , plus the energy gap, E_g . The spectral dependence of the direct excitation process is in agreement with the theoretical model developed by Kane, in which there is a complete absence of scattering either in the bulk or at the surface for those excited electrons which are emitted. The indirect process is also in agreement with Kane's theory. The dependence of the yield on sample doping, in conjunction with the theoretical model, may be used to determine a direct-flight escape depth for excited electrons of $25 \text{ \AA} \pm 5 \text{ \AA}$ for electron energies about 5.5 eV above the valence-band maximum.

I. INTRODUCTION

PHOTOELECTRIC emission from metals has been studied extensively, and it is usually assumed that light absorption leading to photoelectric emission takes place only at the surface of the metal where the electrons are subject to the surface effect. Some recent work on alkali metals,¹⁻³ however, has indicated that photoelectrons can originate at depths below the surface of several hundreds of angstroms. Such observations indicate rather that a volume effect dominates the emission.

The theory that photoelectric emission from semiconductors is a volume effect is generally accepted. The effect of band bending at the surface⁴⁻⁶ and the energy distribution of valence-band density of states⁵⁻⁷ have been discussed theoretically. Recently, some work on cesium-coated silicon surfaces⁸ has substantiated the theoretical expectation that *p*-type samples should exhibit a higher photoelectric quantum efficiency than

n-type samples. Work on alkali antimonides also indicates that photoelectrons can originate at depths well beneath the surface.⁹ These results again indicate that the volume effect must be considered.

Optical excitation leading to photoelectron emission in a volume effect would be subject to the optical absorption selection rules of the lattice and would therefore consist, in general, of an indirect or phonon-assisted transition and a direct transition in which the initial and final electron states differ in **k** vector only by the photon **k** vector.

This paper discusses experimental measurements of photoelectric emission from atomically clean silicon surfaces prepared by cleavage in high vacuum, as a function of the sample doping. The results confirm the dominance of the volume photoelectric effect. As expected, *p*-type samples have a higher yield than *n*-types samples. In addition, the spectral yields from certain resistivity ranges show distinct structure, which is interpreted as the onset of an efficient direct excitation mechanism about 0.3 eV above the lower-energy indirect excitation threshold. The spectral dependence of these two components is determined and the influence of the profile of the space-charge region and the mean free path of the excited photoelectrons is examined.

¹ H. Thomas, Z. Physik **147**, 395 (1959).

² H. Meyers and H. Thomas, Z. Physik **147**, 419 (1959).

³ S. Methfessel, Z. Physik **147**, 442 (1959).

⁴ W. E. Spicer, J. Appl. Phys. **31**, 2077 (1960); R. C. A. Review **19**, 555 (1958).

⁵ L. Apker, E. Taft, and J. Dickey, Phys. Rev. **74**, 1462 (1948).

⁶ D. Redfield, Phys. Rev. **124**, 1809 (1961).

⁷ H. B. Huntington and L. Apker, Phys. Rev. **89**, 352 (1953).

⁸ J. J. Scheer, Philips Research Repts. **15**, 584 (1960).

⁹ W. E. Spicer, Phys. Rev. **112**, 114 (1958).

II. EXPERIMENTAL TECHNIQUES

The silicon surfaces to be examined were (111) faces prepared by cleavage in a vacuum of 1×10^{-10} mm Hg. Surfaces of unusually high quality were obtained by using a special "L"-shaped cross section.¹⁰ Two types of samples were used. On one type, spectral yield as a function of sample doping was studied. These samples had the doping graded along their length and could be advanced and cleaved 10 to 15 times in the same vacuum. On the other type of samples, a direct measure of the yield ratio between *n*- and *p*-type samples was obtained from cleavages which simultaneously exposed both sides of a *p-n* junction. Samples ranged in resistivity from 0.002 to 250 Ω -cm, *p*-type (boron doped) and from 0.0015 to 200 Ω -cm, *n*-type (arsenic doped). Spectra taken on surfaces having particularly poor cleavages showed erratic spectral yields and such data were discarded as unreliable.

The relative specular reflectivity of one of the cleaved surfaces was measured in vacuum over the energy range 4.4 to 6.4 eV. It was found to be in agreement with the results given by Phillip and Taft¹¹ and did not vary by more than 15% over the range of interest for the emission studies. Corrections for this variation have not been made in the treatment that follows.

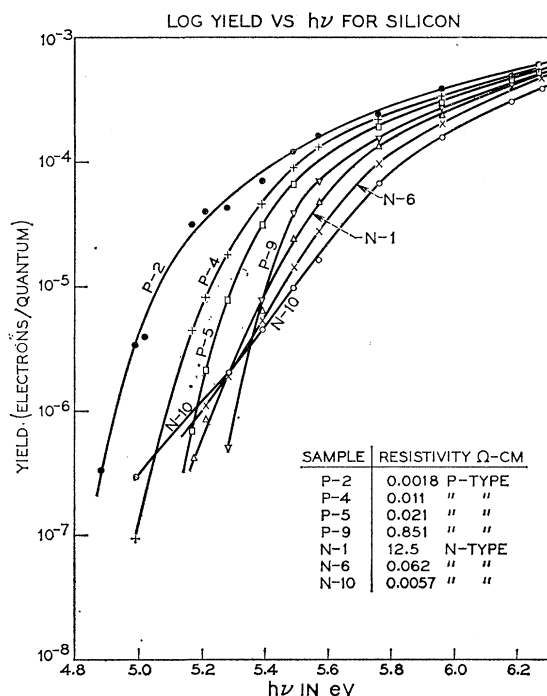


FIG. 1. Log of photoelectric yield in electrons per quantum vs photon energy for cleaved silicon with various impurity concentrations.

¹⁰ G. W. Gobeli and F. G. Allen, J. Chem. Phys. Solids **14**, 23 (1960).

¹¹ H. R. Phillip and E. A. Taft, Phys. Rev. **120**, 37 (1960).

Ultraviolet radiation (1900 to 2700 Å) from a medium pressure, Hanovia SH, mercury arc was passed through a grating monochromator and focused with front-surface mirror optics on the sample at normal incidence. The incident light intensity was continuously monitored by splitting off a portion (about 10%) of the monochromatic beam, focusing this fraction onto a sodium salicylate phosphor,¹² and measuring the phosphor output with an electron multiplier phototube. Absolute intensity was measured by comparison with a CsSb phototube calibrated by Apker and Taft.

The scattered radiation in the tube is reduced by allowing the specularly reflected beam to pass out the same window through which it entered. Spurious emission from surfaces other than those of the sample is eliminated by mounting the sample on insulating clamps and measuring only the current leaving the sample. All other surfaces in the tube serve as the collector. Spurious low photoelectric thresholds were obtained until precautions were taken.

The work function of all samples studied was measured shortly before or after the photoelectric measurements by the Kelvin contact potential difference method.¹³

III. DISCUSSION OF DATA

The results of the contact potential measurements showed that the work function varied only from 4.75 eV to 4.90 eV in covering the entire range from *n* to *p* type with the large changes occurring at the extreme resistivities.¹³ The work function of high-resistivity samples was 4.82 eV. This, together with the best estimate for the indirect threshold of 5.15 eV indicates that the Fermi level at the surface is about 0.33 eV from the top of the valence band for samples of high resistivity, and moves up and down only about 0.1 eV in going to either extreme in doping. The flat-band condition will therefore occur in samples having a bulk Fermi level about 0.33 eV above the valence band edge, i.e., about 500 Ω -cm *p* type.

Figure 1 is a plot of the log of the yield in electrons per incident quantum as a function of photon energy for sample dopings ranging from extreme *n* to extreme *p* type.

Two general features of the data are clearly seen: (1) the yield increases as the samples become more *p* type, and (2) as the samples become extremely *n* type, a "tail" begins to grow in the low-energy region of the yield spectrum.

In explaining these effects, it is first pointed out that photoelectric emission from a semiconductor, in general, can arise from electrons in the valence band, in the conduction band, or in surface states. Changing the bulk doping moves the Fermi level at the surface through a small energy range, which will cause predict-

¹² K. Watanabe and E. C. Y. Inn, J. Opt. Soc. Am. **43**, 32 (1953).

¹³ F. G. Allen and G. W. Gobeli, Phys. Rev. **127**, 150 (1962).

able effects on the emission in each of these three cases. We can assume¹⁸ in the following that changes in χ , the electron affinity due to bulk doping, are small for all but the most degenerate samples.

Emission from surface states should either increase as the surface is made more *n* type and decrease as it is made more *p* type, or else remain constant in both cases, depending upon the presence or absence of surface states near the Fermi level at the surface.

Considering now the second of the above features of the data we see that the *n*-type "tail" emission could arise from surface states, since it does increase with an increasing *n*-type bulk. Emission from the conduction band might also account for this emission as follows: since the surface position of the Fermi level is nearly constant, it is possible for very high *n*-type dopings that the conduction band bends up very sharply to the surface. If the electron concentration in the conduction band reaches sufficiently high values within an escape depth of the surface, emission from the conduction band should become observable. This emission would have a photoelectric threshold equal to the work function and would increase as the donor concentration increased. However, it is found that this low-energy "tail" begins to increase appreciably in *n*-type samples having $\sim 10^{17}$ donors/cm³. Such samples have a space-charge depth of several hundreds of angstroms and the Fermi level is still over 0.1 eV below the conduction band in the bulk. Therefore, the electron concentration would not reach appreciable values close enough to the surface to permit measurable emission from the filled conduction band states. We, thus, interpret the yield in the low-energy tail for *n*-type samples as arising from surface states in which the electron population is increasing as the samples become more *n* type.

The data are not accurate enough to allow a detailed analysis of this surface state emission. For 10^{19} donors/cm³, the yield has an approximate magnitude of 2×10^{-6} electrons/quantum at $h\nu = 5.2$ eV and the magnitude decreases by a factor of 5, when the impurity concentration changes from 3×10^{19} cm⁻³ to 2.5×10^{17} cm⁻³. If this order of dependence is maintained to lower donor concentrations, the yield from this process at 5.2 eV for an intrinsic sample would be less than $\sim 10^{-9}$ electrons/quantum and would be totally unobservable. For the flat band samples, which have high resistivity *p*-type surfaces as has been shown, this type of surface state emission could not affect the results in any way which might lead to ambiguities in the interpretation. The important point is that this emission clearly arises from a different mechanism than the dominant, higher energy process and that it can be neglected in the following discussion and interpretation.

Returning to the first and dominant feature of the data, the increasing yield as samples become more *p* type,—it is seen that this could not be explained by emission from surface states, because the doping dependence is in the wrong direction. This higher yield

for *p*-type samples and the spectral shape changes with doping can be accounted for by the influence of space-charge band bending on volume photoelectric emission from the valence band. The dominant effect of this band bending is to raise or lower the effective photoelectric threshold for electrons originating from increasing depths below the surface. If the maximum depth of origin is comparable to, or greater than the space-charge depth, an appreciable fraction of the emission is characteristic of a raised or lowered threshold.

From Fig. 1 it is seen that yield increases as sample doping goes from *n* to *p* type over the entire range of samples, disregarding the low-energy *n*-type tail. Measurements of the yield ratio were made directly across the *p-n* junctions exposed by cleaving and gave a value of ~ 2.1 at $h\nu = 6.0$ eV for the most degenerate *p*- to most degenerate *n*-type samples. Due to the possibility of light scattering onto the high yield side, this must be regarded only as a lower limit for this ratio. Results on graded crystals indicate the value of this ratio may be as high as 6. However, the accuracy is sufficient to establish the family of curves shown in Fig. 1.

Figure 2 gives the plot of square root of yield as a function of photon energy for atomically-clean, single-crystal tungsten, for high-resistivity silicon and for heavily doped *n*- and *p*-type silicon. The tungsten data fall on a straight line (except for the expected small deviation a few kT from the threshold) as has been observed by many other workers and predicted by the Fowler plot form. The curve for the high-resistivity *p*-type sample is typical of those obtained over a large range of higher resistivities ($\rho > 1$ Ω -cm), both *n* type and *p* type. Deviations from this curve occur slowly as the resistivities go toward low values and proceed rapidly at very low resistivity values reaching the limiting forms shown in Fig. 2 for the heavily *p*-type and *n*-type samples, respectively.

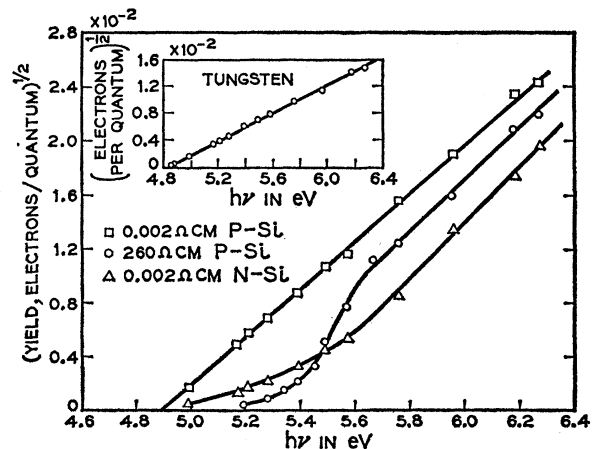


FIG. 2. Square root of yield vs photon energy for clean single-crystal tungsten (orientation $\sim [113]$) and for typical cleaved silicon samples.

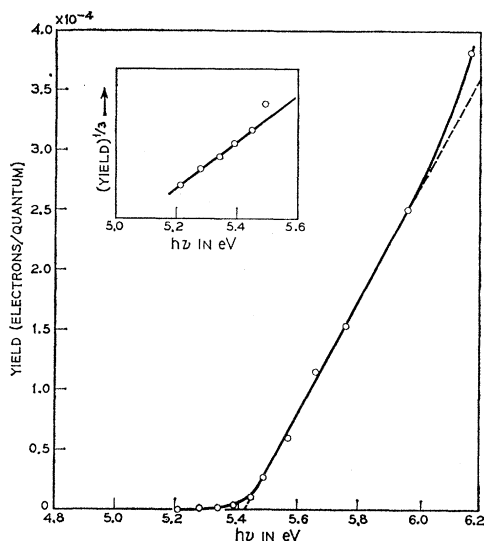


FIG. 3. Linear plot of yield vs photon energy for 250 Ω -cm *p*-type silicon. Inset shows cube root plot for low-energy points. See Sec. V for comment on determination of indirect threshold.

Since the absorption depth of the ultraviolet radiation is about 60 Å in this spectral range,¹¹ the effects of band bending will be observable only for samples in which the bands can bend appreciably in this distance. The 250 Ω -cm, *p*-type sample of Fig. 2, which has a space-charge depth of many thousands of angstroms, fulfills the requirement that there is *no* appreciable band bending in this distance. The spectral yield of this sample is therefore typical of the flat-band emission which will be discussed in detail. Analyses of the spectral yield shape for the high-resistivity sample on the basis of a conventional power law theory involving a single emission process were unsuccessful. The fact that this spectral yield curve consists of two distinct components is strikingly demonstrated in Fig. 3 where a linear plot of the yield as a function of photon energy is given. The sharply-rising linear portion of the yield curve which extrapolates to a "threshold" of 5.45 eV is characteristic of samples covering the high-resistivity range.

The insert in Fig. 3 shows a cube root plot of the data at lower photon energies and indicates that the low-energy tail approximately follows a cube power law. Analysis of many samples indicates that this power law is subject to some uncertainty arising from small differences in the perfection of the cleavage faces. These differences and the low yield in this spectral region, which make accurate measurements difficult, cause the best fit for various higher resistivity samples to be somewhat uncertain. Thus, the empirical cube law dependence must be regarded as a good approximation.

On the basis of the above observations, the following conclusions may be drawn: (1) The dominant emission is a volume process and arises from excitation from the valence band which is modified by band bending at the surface due to space-charge effects; and (2) this

dominant emission consists of two components: a linear component of high relative efficiency having an extrapolated threshold of 5.45 eV, which we identify as the direct transition threshold, and a component obeying approximately a cube law of relatively low efficiency having an extrapolated threshold in the neighborhood of 5.1 eV, which we identify as the indirect transition threshold.

Based on these conclusions, a detailed model can now be constructed.

IV. THEORETICAL MODEL

First, consider the emission from a pure semiconductor which has the valence band flat to the surface. The theory of photoelectric emission from such a semiconductor sample is discussed by Kane.¹⁴ Two excitation processes were considered; one arising from direct optical absorption and the other from indirect absorption. A variety of specular dependencies are predicted in each case depending on the specific assumptions made concerning the scattering mechanisms affecting the excited electrons.

The high-intensity, linear component which we observe can arise only for the direct optical excitation process and only when there is a complete absence of any sort of scattering of the excited carriers, either in the volume of the material or at the surface.

This absence of scattering at the surface suggests that the perfection of surfaces exposed by careful cleavage in high vacuum is probably quite good since a seriously distorted surface layer should be an efficient source of scattering.

The empirical power law,

$$y = c_i(h\nu - h\nu_i)^3, \quad (1)$$

is in agreement, within experimental accuracy, with the predicted 5/2 power law for the volume indirect excitation process. This is also the power law dependence for a surface process with an imperfect surface acting as a momentum absorber. However, the experimental data are not consistent with detailed computations, described in Sec. V, based on the assumption of a surface phenomenon. Thus, the volume indirect process accounts for the observed lower-energy emission.

The erratic behavior observed for poor cleavages (see Sec. II) is probably due to increased scattering at the surface resulting from the cleavage imperfections. Such scattering would decrease the amount of direct photoelectric emission observed. Any electrons removed from the direct process by scattering could appear to some degree as indirect photoelectrons and would thus enhance the low-energy emission. Even on the better samples, small deviations from perfection in the surfaces could well have measurable effects on the direct photoelectric yield and could explain the variations in the

¹⁴ E. O. Kane, Phys. Rev. **127**, 131 (1962).

experimentally observed yield ratio between extreme *n*- and *p*-type samples at 6.0 eV.

The case of emission from a flat band sample and the effect of band bending on the yield spectrum are discussed with reference to Fig. 4.

Figure 4(b) is the usual energy vs depth diagram in which the top of the valence band at the surface ($x=0$) is taken as the zero of energy. The adjacent E vs k diagram of Fig. 4(a) for a simple hypothetical two-band semiconductor is drawn with the same energy scale. The maximum of the valence band V lies at $k(0,0,0)$ as does the minimum of the C band. Thus the minimum separation between the bands is a direct energy gap of magnitude E_d , which is shown less than the height of the vacuum level. The energy required to raise an electron from the top of the valence band at the surface to the vacuum level is defined as the photoelectric threshold, Φ .

The difference between the direct and indirect thresholds is only 0.3 eV. It is shared between the kinetic energy of the hole and the transverse kinetic energy of the emitted photoelectron at threshold and such a small value certainly indicates that the threshold lies on the $[111]$ direction or at least very close to it. The actual band structure of silicon in this energy region is known to be much more complicated than shown in this simple model. According to Phillips' calculations,¹⁵ there are three conduction bands (the L_1, L_2, L_3 bands) which have minima at $k(0,0,0)$ about 4 eV above the valence band maximum. Two of these bands also have a maxima in the $[111]$ direction, possibly near the energy range of interest for the photoelectric experiments. However, the complexity of the situation does not invalidate the conclusions reached concerning the direct and indirect emission processes. Further experiments, in which the electron affinity of the samples is lowered, (e.g. by the adsorption of Cs^+ ions) could well yield valuable information on the band structure of semiconductors throughout this higher energy range.

The photoelectron must be excited into a final state of band C which lies above the vacuum level. For the indirect transition, in which phonon interactions conserve momentum, transitions between arbitrary states of the V band and the C band are possible provided only that they are energetically permissible. Thus, the indirect transition threshold $h\nu_i(0)$ is just the energy required to raise an electron from the top of the valence band, $E_v(0,0,0)$, at the surface of the sample to the vacuum level and is by definition the photoelectric threshold, Φ . That is,

$$h\nu_i(0) = E_d + \epsilon_c(\mathbf{k}_\Phi) = \Phi. \quad (2)$$

\mathbf{k}_Φ is defined as the value of \mathbf{k} along the $[111]$ direction at which the vacuum level intersects the C band. For a direct transition, the \mathbf{k} vector of the excited electron's initial and final state differs only by the

¹⁵ J. C. Phillips, Phys. Rev. **125**, 1931 (1962). See earlier papers, e.g., L. Kleinman and J. C. Phillips, Phys. Rev. **118**, 1153 (1960).

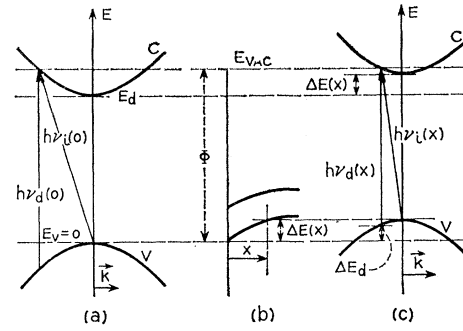


FIG. 4. Energy vs k and energy vs depth diagram for a simple two-band semiconductor.

(negligible) photon \mathbf{k} vector. Specification of the final state in the C band also fixes the initial state in the V band. The direct transition threshold is the energy required to raise a valence band electron at $\mathbf{k}=\mathbf{k}_\Phi$ into a C -band state of the same \mathbf{k} vector.

The direct photoelectric threshold is given by

$$h\nu_d(0) = E_d + \epsilon_c(\mathbf{k}_\Phi) + \epsilon_v(\mathbf{k}_\Phi) = h\nu_i(0) + \epsilon_v(\mathbf{k}_\Phi). \quad (3)$$

Thus, the direct photoelectric threshold, in general, lies at a higher energy than the indirect threshold.

On this basis it is expected that the spectral yield should rise from the indirect photoelectric threshold and then show an abrupt increase as the direct photoelectric threshold is exceeded and the more efficient process dominates. This is clearly the observed behavior.

The total emission can be written

$$y = c_i(h\nu - h\nu_i)^{\frac{1}{2}} + c_d(h\nu - h\nu_d), \quad (4)$$

where c_i and c_d are constants containing the light intensity and the absorption efficiencies for production of excited electrons with final states lying above the vacuum level.

Consider now the effect of depth beneath the surface at which the excited electrons are created. As shown in Fig. 4b, the distance from the top of the valence band to the vacuum level, which defines the indirect photoelectric threshold, varies as a function of x for the case of a sample having bands bent down to the surface. The corresponding changes in the quantities $h\nu_i$ and $h\nu_d$ as a function of x are shown. Thus, in Eqs. (3) and (4) the thresholds are functions of x and should be written as $h\nu_i(x)$ and $h\nu_d(x)$.

The attenuation of the incident light and the escape depth of the excited electrons must both be considered. For the light intensity the normal exponential attenuation factor is used characterized by an absorption depth l_α [$l_\alpha = 1/\alpha = 1/(1.6 \times 10^6) = 60 \text{ \AA}$ for Si near $h\nu = 5.5 \text{ eV}$].¹¹

The mean free path of the electrons is less well known and an exponential attenuation factor characterized by an escape depth l_e is used.

As is pointed out by Kane, the direct-excitation photoelectric threshold occurs along a high-symmetry

direction, e.g., [111]. Near the threshold, electrons are excited into states characterized by velocities directed into a small angle cone whose axis is normal to the surface. Even purely elastic collisions which merely deflect such excited electrons away from the surface must be considered as scattering processes. Thus, l_e is a direct-flight escape depth as distinguished from a diffusion escape depth in which the excited electrons could suffer one or more collisions involving small energy losses and still escape over the surface barrier. It should also be borne in mind for future refinements in both experimental accuracy and interpretation that the escape depth is probably different for the direct and indirect processes. In addition, l_e may be expected to depend upon $h\nu$ when large ranges of energy are involved.

Thus, we have

$$y(h\nu, x) = c_i [h\nu - h\nu_i(x)]^{\frac{5}{2}} e^{-x/l} + c_d [h\nu - h\nu_d(x)] e^{-x/l}, \quad (6)$$

where $1/l = (1/l_a) + (1/l_e)$ and the thresholds are dependent on the depth beneath the surface. In both cases the thresholds will have the form

$$\begin{aligned} h\nu_i(x) &= h\nu_i(0) - \Delta E(x), \\ h\nu_d(x) &= h\nu_d(0) - \Delta E(x) - \Delta E_d(x, \mathbf{k}) \\ &= h\nu_d(0) - b\Delta E(x), \end{aligned} \quad (7)$$

where $b = 1 - (dE_c/dk)/(dE_v/dk)$ and $\Delta E(x)$ is the profile of the valence band as a function of depth beneath the surface. The measured yield may be obtained by integration over the depth

$$\begin{aligned} Y(h\nu) &= c_i \int_0^\infty [h\nu - h\nu_i(0) + \Delta E(x)]^{\frac{5}{2}} e^{-x/l} \frac{dx}{l\alpha} \\ &\quad + c_d \int_0^\infty [h\nu - h\nu_d(0) + b\Delta E(x)] e^{-x/l} \frac{dx}{l\alpha}. \end{aligned} \quad (8)$$

The integration is carried out only for those values of x which, for a given $h\nu$, yield a positive value for the integrands and in all cases states above the Fermi level are assumed to be empty and states below are assumed to be occupied by electrons.

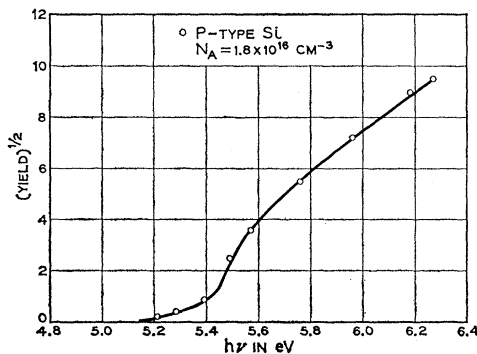


FIG. 5. (Yield in arbitrary units) $^{1/2}$ vs $h\nu$. Solid curve is calculated from Eq. (8) for flat-band condition and $l_e = 25$ Å. Points are experimental data normalized to calculated curve at $h\nu = 5.96$ eV.

V. ANALYSIS OF DATA

The term $\Delta E(x)$ of Eq. (8) may be determined for the various samples by a numerical integration of Poisson's equation using the surface potential, bulk potential, and impurity concentrations. In most of the cases of interest (very high impurity concentrations) the general form of the solution is required and the difficult problem of obtaining a smooth transition in these solutions between the classical, nondegenerate case and the extremely degenerate case is discussed in the Appendix.

Both the potential profile $\Delta E(x)$ and the solution for Eq. (8) were solved numerically with the aid of an IBM 7090 digital computer.

The value of $h\nu_d(0)$ was found from linear extrapolation of the data for several samples to be 5.45 ± 0.03 eV. The value of $h\nu_i(0)$ could not be so clearly defined from the experimental data. It was determined to be 5.10 eV from the best cube law fit to the yield near threshold for several high-resistivity samples where space-charge band bending was not important. $h\nu_i(0)$ was also determined by the quality of fit for all data to the solution of Eq. (8). Employing this $5/2$ power law for the spectral dependence, the value of $h\nu_i(0) = 5.15$ eV gives the best fit and this value has been taken as the most reliable. The uncertainty in $h\nu_i(0)$ is ± 0.08 eV.

The ratio c_d/c_i was determined to be 4.5 (for energies in volts) from the spectral yield curve for a sample with 1.5×10^{16} acceptors/cm 3 . This sample has a very gradual variation in the space-charge profile in addition to having a bulk Fermi level very close to the surface Fermi level. Thus, its spectral yield curve is representative of the flat-band condition. The solid line of Fig. 5 is a plot of Eq. (8), for the flat-band case of $\Delta E(x) = 0$ and $c_d/c_i = 4.5$. The experimental data for the high-resistivity sample are normalized to this theoretical curve at one point and the agreement for the assumed ratio is quite satisfactory, as can be seen from the plotted points.

The parameter b is the most uncertain factor in Eq. (8). We expect b to be of order of magnitude unity. The fit of Eq. (8) to the data was found to be rather insensitive to the choice of b . The final value of $b = 1.5$ was judged to be a somewhat better fit than either 1.0 or 2.0.

The remaining parameter, l , involving the escape depth of excited electrons, was found to have a large effect on the shape and magnitude of the spectral yield curves. In fact, the fit to Eq. (8) is good enough so that the data may be used to determine the escape depth of the excited (photo) electrons.

Fig. 6 shows several calculated spectral yield curves for a p -type sample with 4.4×10^{18} acceptors/cm 3 as a function of the escape depth, l_e . The curves were normalized at $h\nu = 6.0$ eV in order to illustrate the shape dependence of l . The solid points are experimental data for the sample and indicate that a value of l_e somewhat greater than 20 Å, but less than 30 Å, gives the best fit.

The value of l_e was then chosen to be 25 Å and the yield curves for all samples measured were computed from Eq. (8). The agreement between experiment and theory was quite satisfactory for all samples and Fig. 7 shows the computed curves and experimental points for samples of widely differing impurity concentrations.

The disagreement at low-photon energies in the n -type samples is expected as a result of the process tentatively identified as surface-state emission discussed in Sec. III, for which no provision has been made in this theoretical model. The calculated curves predict that the yield at $h\nu=6.0$ eV for the p -type sample with 8.5×10^{18} acceptors/cm³ is 2.25 times the yield for the n -type sample with 9.5×10^{18} donors/cm³. This is consistent with the experimental determination as discussed in Sec. III.

Finally, the total yield of $\sim 4 \times 10^{-4}$ electrons/quantum observed at $h\nu=6.0$ eV for the pure sample

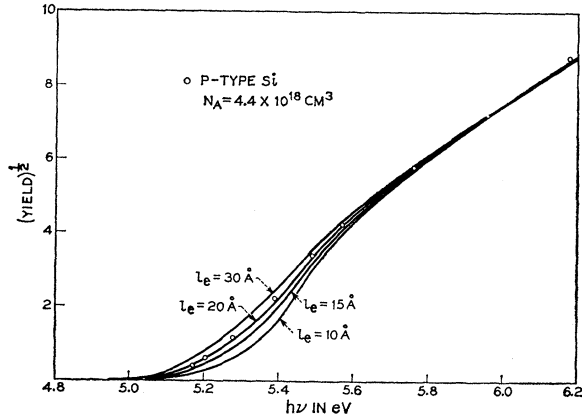


FIG. 6. (Yield in arbitrary units)^{1/2} vs $h\nu$. Solid curves are calculated from Eq. (8) for the indicated values of l_e . Points are experimental data normalized to calculated curve at $h\nu=5.96$ eV.

appears at first glance to be unusually low for a direct-excitation volume process, especially under the assumption that there is no scattering of the excited electrons. A *crude* estimation of the expected yield for the direct transition process with no scattering of emitted electrons may be obtained from the following expression for the yield

$$Y = (1-R)(l_e/l_e + l_a)(1-p_s) \times \frac{g_v \pi k^2 / (dE/dk)}{\sum_{i,j} \int \delta[h\nu - E_i(\mathbf{k}) + E_j(\mathbf{k})] d\mathbf{k}} \quad (9)$$

R is the reflectivity of the surface and is equal to 0.65 for photon energies near 5.5 eV.

The term $l_e/(l_e + l_a) = 25 \text{ Å} / (25 \text{ Å} + 60 \text{ Å}) = 0.3$ is the quantitative expression for the fraction of absorbed light

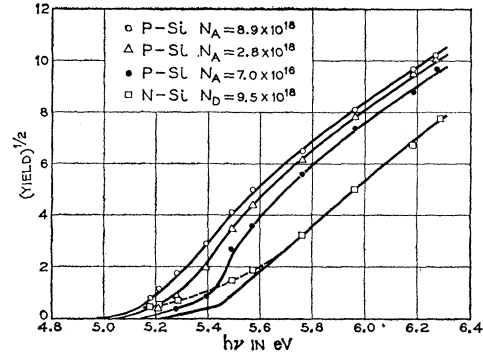


FIG. 7. (Yield in arbitrary units)^{1/2} vs $h\nu$. Solid curves are calculated from Eq. (8) with $l_e=25$ Å. Points are experimental data normalized to the calculated curve at $h\nu=5.96$ eV.

that is effective as a result of the escape depth being smaller than the absorption depth of the light.

The term $(1-p_s)$ is the fraction of the excited electrons reaching the surface which escape without scattering. Since the surfaces in question are of very high quality, we shall assume that nearly all of such electrons are transmitted, i.e. $p_s=0$.

The last term is the precise expression for the direct-excitation, no-scattering, theoretical model which replaces the escape-probability or solid-angle-for-escape terms of earlier theories. The optical matrix element is assumed to be roughly constant and therefore has been canceled.

The integral of $\delta[h\nu - E_i(\mathbf{k}) + E_j(\mathbf{k})]$ defines the optical energy shell for direct transitions between two bands and the summation indicates that several final and initial bands may contribute to the over-all absorption. We assume that excitation into only one upper band leads to emission of photoelectrons and the factor g_v takes into account that more than one initial state band can contribute. In our case $g_v=2$ because of the double degeneracy of the valence band in silicon. The remaining term in the numerator represents that part of the optical energy shell which fulfills the conditions for emission.

Since it is known that at least three upper state bands could be effective in the band to band absorption¹⁵ in this spectral region we shall use a factor of 6 in the denominator for the summation over the two possible initial states and the three possible final states.

The size of the optical energy shell is unknown but it is presumably of the order of the Brillouin zone. Thus, we shall write

$$Y = (1-R) \left(\frac{l_e}{l_e + l_a} \right) (1-p_s) \frac{\pi k^2 / (dE/dk)}{3(4\pi K^2) / \langle dE/dk \rangle_{av}}, \quad (10)$$

where $4\pi K^2$ is the area of a sphere with radius equal to half the dimension of the first Brillouin zone in silicon. We shall assume that dE/dk and $\langle dE/dk \rangle_{av}$ are not greatly different and they therefore will cancel.

The appropriate value of k may be determined from the expression for the kinetic energy of the emitted electron

$$\hbar^2 k^2 / 2m = \mathcal{E}(\hbar\nu), \quad (11)$$

where m is the free electron mass.

We shall make the *crude* approximation

$$\mathcal{E}(\hbar\nu) = \hbar\nu - \hbar\nu_d(0). \quad (12)$$

Taking $K \cong 10^8 \text{ cm}^{-1}$,

$$\hbar\nu - \hbar\nu_d(0) = 6.0 - 5.45 = 0.55 \text{ eV}, \quad (13)$$

we obtain a value of 0.04 for the remaining term of Eq. (10). Thus, the estimated value of the yield is

$$Y = \frac{(0.35)(0.30)(1.0)(0.04)}{3} = 1.4 \times 10^{-3} \text{ electrons/incident quantum}, \quad (14)$$

which would indicate that the observed yield is not unreasonably low. It seems likely that the disagreement between this value and the experimental value is contained in the estimation of the last factors of Eq. (9), although it could conceivably be contained in the surface scattering factor, $(1 - p_s)$.

In view of the good agreement of experimental data for all impurity concentrations with the theoretical model, the following conclusions may be drawn, in addition to those given at the end of Sec. III.

The direct photoelectric emission process is a volume process with a complete absence of scattering of the observed electrons either in the volume *or at the surface*.

The details of the dependence of yield on sample impurity concentration may be accounted for quantitatively by the effects of space-charge band bending at the surface on volume excitation from the valence band.

An emission process becomes observable at low energies for strongly n -type samples that is probably emission from filled surface states.

The escape depth of excited electrons in silicon is $25 \text{ \AA} \pm 5 \text{ \AA}$ for electrons about 5.5 eV "hot" relative to the top of the valence band.

It must also be emphasized that this is a direct-flight escape depth since there is no scattering involved and it cannot be considered as a diffusion escape depth.

In general, the model discussed by Kane,¹⁴ based on volume excitation with no scattering of the excited electrons, is supported by the experimental data.

ACKNOWLEDGMENTS

The authors wish to thank E. O. Kane for helpful comments and suggestions throughout the course of this work, and A. A. Studna for his technical assistance.

APPENDIX

The electric field in a semiconductor at a point x is obtained by integrating Poisson's equation and is given

by

$$\frac{du(x)}{dx} = \pm \left\{ \frac{8\pi e}{kT} \int_{u(x)}^{u(\text{Bulk})} \rho(u) du \right\}^{\frac{1}{2}}, \quad (A1)$$

where the energies are taken relative to the intrinsic Fermi position, $u = (E_F - E_I)/kT$.

The expression for the charge density contains free charge carrier terms and fixed impurity-ion terms. The expression given by Seiwatz and Green¹⁶ is valid for moderate impurity concentrations, such that the impurity atoms do not interact appreciably with one another and thus retain an identity as localized energy states.

The present case of interest lies in the higher impurity concentration range. The impurity activation energy has been appreciably lowered by this interaction between impurity atoms and the impurity states have started to merge into the free-carrier band edge. In the very high-impurity regions, where the impurity states have completely merged into the free-carrier band, experimental evidence indicates that each impurity atom added to the semiconductor produces one free carrier,¹⁷ and therefore each added impurity atom becomes a charged ion.

It is possible to make a smooth transition between the low-impurity case given by Seiwatz and Green, and the degenerate high-impurity case using a mathematical method which makes physical sense and describes in an approximate way what must be taking place. As the impurity concentration increases, the energy states begin to interact with each other and the "smear" out in energy. The activation energy starts to decrease and slowly a larger and larger fraction of the impurity sites lose their identity as localized states and merge into the band edge.

A variable, $F(N)$, dependent on impurity concentration shall be defined which specifies the fractional number of impurities which retain their discrete character. Thus, $1 - F(N)$ is the fraction of impurities which merge with the free-carrier band and become ionized.

The generalized expression for charge density becomes

$$\rho = |e| \left\{ \frac{F_D N_D}{1 + g_D e^{(E_F - E_D)/kT}} - \frac{F_A N_A}{1 + g_A e^{(E_A - E_F)/kT}} + (1 - F_D) N_D - (1 - F_A) N_A + 4\pi \left(\frac{2kT}{\hbar^2} \right) \times \left[(m_p^*)^{\frac{3}{2}} F_{\frac{3}{2}}(W_{V,I} - u) - (m_n^*)^{\frac{3}{2}} F_{\frac{3}{2}}(u - W_{C,I}) \right] \right\}. \quad (A2)$$

Note that by allowing $F(N)$ to go to zero the degenerate

¹⁶ R. Seiwatz and M. Green, J. Appl. Phys. **29**, 1034 (1958).

¹⁷ R. Logan, E. Gilbert, and F. Trumbore, J. Appl. Phys. **32**, 131 (1961).

case is obtained, and when $F(N)=1.0$ the classical case is obtained.

As a first approximation, it is expected that the function $F(N)$ would show the same functional dependence on impurity concentration as is observed for the activation energy since they are manifestations of the same phenomenon.

The empirical expression,

$$E_i = E_0 - kN^{\frac{1}{3}}, \quad (\text{A3})$$

observed for donors and acceptors in Ge and Si is a reasonable concentration dependence in that $N^{-\frac{1}{3}}$ gives the average impurity-atom nearest-neighbor distance in the crystal.¹⁸ Thus, we shall assume that $F(N)$ has the form

$$F(N) = 1 - k_1 N^{\frac{1}{3}}. \quad (\text{A4})$$

A negative value for either E_i or $F(N)$ does not have physical meaning and it is assumed that both are constant and equal to zero for impurity concentrations in excess of a critical concentration N_c defined by

$$k_1 N_c^{\frac{1}{3}} = 1. \quad (\text{A5})$$

For silicon the accepted value for g_A including the

acceptor ground-state degeneracy is 4.¹⁹ The case of the donor state is complicated by a partial lifting of the ground-state degeneracy due to the valley-orbit splitting. The value of g_D should be determined from the expression

$$g_D = 2(1 + 5e^{-\Delta/kT}), \quad (\text{A6})$$

where Δ is the valley-orbit splitting between the symmetrical lowest energy total wave function and the other five combinations of the individual wave functions.

For arsenic in silicon, Δ may be estimated to be 0.018 eV from effective mass energy consideration,²⁰ yielding $g_D=7.0$ at room temperature.

It was necessary to obtain values of $u(x)$ as a function of depth beneath the surface, which were obtained by an iterative numerical solution of the differential equation [Eq. (15)] using a program for an IBM 7090 digital computer. The program gives results in good agreement with those of other workers in regions of over-lapping applicability and in addition gives a progressive family of curves as the "transition region" is encountered.

¹⁹ H. Brooks, *Advances in Electronics and Electron Physics*, edited by L. Marton (Academic Press Inc., New York, 1955), Vol. 7, p. 118.

²⁰ W. Kohn, *Solid State Physics*, edited by F. Seitz and D. Turnbull (Academic Press Inc., New York, 1957), Chap. V, p. 297.

¹⁸ W. Shockley, *Electrons and Holes in Semiconductors* (D. Van Nostrand Company, Inc., Princeton, New Jersey, 1950), p. 228.